Available online at www.sciencedirect.com

SciVerse ScienceDirect

Ceramics International 38 (2012) 1671–1675

CERAMICS INTERNATIONAL

www.elsevier.com/locate/ceramint

Simple synthesis and characterization of mesoporous (N, S)-codoped TiO_2 with enhanced visible-light photocatalytic activity

Nian Yao [a], Congcong Wu [a], Lichao Jia [a], Song Han [b], Bo Chi [a,*], Jian Pu [a], Li Jian [a]

[a] School of Materials Science and Engineering, State Key Lab of Material Processing and Die & Mould Technology, Huazhong University of Science and Technology, Wuhan, Hubei 430074, China

[b] College of Forestry, Northeast Forestry University, Harbin 150040, China

Received 17 June 2011; received in revised form 23 September 2011; accepted 28 September 2011
Available online 5 October 2011

Abstract

Mesoporous (N, S)-codoped TiO_2 was simply prepared by a solvothermal method with thiourea as N and S source. The as-prepared products were characterized by XRD, SEM, XPS, BET and UV–vis. The results confirm that N and S have been incorporated into the lattice of anatase TiO_2, which brings an obvious red-shift of the absorption edge into visible-light region. Moreover, the codoped products exhibit high photocatalytic activity under the visible-light irradiation.

Keywords: Anatase; N, S-codoping; Mesoporous; Visible-light photocatalyst

1. Introduction

For the application as photocatalyst, titania (TiO_2) has attracted comprehensive scientific interests and been widely investigated in recent years, due to its advantages such as low lost, nontoxicity, availability, and structural stability [1–8]. However, TiO_2 can only be activated under the UV light irradiation for its wide band gap (3.2 eV), which means that a red-shift of the absorption edge to visible-light region is quite necessary in order to fully utilize the solar light. Recently, many efforts have been made to shift the absorption spectrum of titania towards the visible-light region. Among these efforts, the doping of ions, especially anions doping as N, F, S, B, and C anions, has been proved to be effective doping ions in TiO_2 through mixing their p orbits with the O 2p orbits in TiO_2 to reduce the band gap energy of TiO_2 [9,10]. Furthermore, it has been confirmed that the codoping of multiple ions can further extend the absorption edge into the visible-light range and promote the efficiency of photocatalysis obviously because of the synergistic effect of the multiple ions [11–16].

TiO_2 with mesoporous structure has also been used as an efficient photocatalyst for the decomposition of the organic compounds and in dye-sensitized solar cells for its large surface area and pore volume [17–19]. Usually, mesoporous TiO_2 is prepared by template-based methods using soft templates (surfactant and block polymers) or hard templates (porous silica, polystyrene spheres, and porous carbon) [20–23]. For the hard templates, the complete removing of these templates will be difficult. And most of the soft templates are organic molecules, which are favorable to form super mesoporous structure. However the removal of the organic templates would bring environment problems [24].

In this paper, a simple solvothermal method is used to synthesize the (N, S)-codoped anatase phase TiO_2 with mesoporous structure. In the typical synthesis process, tetrabutyl orthotitanate (TBOT) is used as the precursor and thiourea as the sources of the nitrogen and sulfur doping. The result shows that in this process, (N, S)-codoped anatase TiO_2 with mesoporous structure can be obtained without the existing of any hard or soft templates. It is found that the thiourea not only can provide the codoping sources, but also help to form TiO_2 spheres with mesoporous structure by adjusting the pH value of the solution during the solvothermal treatment. The photocatalytic activities are evaluated by the photodegradation of methylene blue (MB) under the visible-light irradiation, which

* Corresponding author.
E-mail address: chibo@hust.edu.cn (B. Chi).

0272-8842/$36.00
doi:10.1016/j.ceramint.2011.09.059

confirms that the as-prepared (N, S)-codoped TiO_2 shows enhanced visible-light photocatalytic activity.

2. Experimental details

2.1. Synthesis of materials

The (N, S)-codoped mesoporous TiO_2 spheres were prepared by a solvothermal method. 0.003 mol TBOT was mixed with 4 g HCl (37 wt%), and thiourea was mixed with 30 mL ethanol (99.5%), respectively. Then the latter mixture was slowly put into the former one under continuously stirring. After stirring for 2 h, the obtained transparent solution was transferred into the Teflon-lined stainless steel autoclave and heated at 150 °C for 6 h. The obtained precipitate was separated by centrifugation and washed with ethanol. Finally, the white powder was annealed at 450 °C for 2 h with a heating rate of 2 °C/min. The molar ratio of thiourea to TBOT was chosen as 0, 0.25, 0.5, 1.0, and 1.5. The corresponding annealed final products were named as NST-000, NST-025, NST-050, NST-100, and NST-150, respectively.

2.2. Measurements

The crystal phases of the products were detected by X-ray diffractometer (XRD, X'Pert PRO) with a Cu Kα radiation. The microstructure was characterized by environment scanning electron microscopy (ESEM, Quanta 200) and field emission scanning electron microscopy (FESEM, Sirion 200). The binding energy was identified by X-ray photoelectron spectroscopy (XPS, Shimadzu ESCA 750). The BET and BJH results were calculated according to N_2 adsorption–desorption measurements at 77 K (Micromeritics ASAP 2020 M analyzer). The shift of absorption edge was measured by the UV–vis diffused reflectance spectra, in which $BaSO_4$ was used as the reflectance standard.

2.3. Photocatalytic activity

The photocatalytic activities of the products were evaluated by the degradation of methylene blue (MB) under visible-light irradiation. A 500 W xenon lamp with a filter (420–750 nm, Trans 95%) was used as the visible-light source. An amount of photocatalyst (0.015 g) was added into a 25 mL MB aqueous solution (2.5×10^{-5} mol/L). Before the photocatalytic experiment, the suspension was stirred in the dark for 0.5 h. The concentration of MB was monitored every 1 h by measuring the maximun absorbance of MB at 664 nm using UV–vis spectrum.

3. Results

3.1. Characterization of (N, S)-codoped TiO_2

Fig. 1 shows the XRD patterns of the as-prepared products. It can be found that most of the products are pure anatase phase, including the unannealed product. It has been reported that the anatase phase is beneficial for the photocatalytic degradation in many relevant studies. From Fig. 1, it also can be found that the characteristic peaks belongs to rutile are also existing in the undoped (a) and NST-025 (b) samples. However, with the increasing of the thiourea in the starting materials, the products gradually exhibit homogeneous pure anatase phase. The result shows that the doping may prevent the formation of rutile structure and result in the formation of the pure anatase structure.

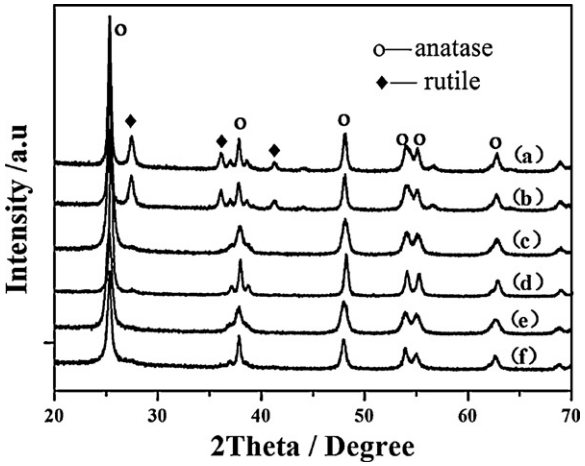

Fig. 1. XRD patterns of as-prepared TiO_2 structure: (a) NST-00, (b) NST-025, (c) NST-050, (d) NST-100, (e) NST-150, and (f) unannealed product of NST-100.

Fig. 2 shows SEM images of the as-prepared products. SEM images reveal that the prepared TiO_2 powders are mainly composed of irregular small particles of hundreds nanometers and single-dispersed spheres with size of about 1–3 μm. The ratio of particles and spheres changes with different synthesis parameters. According to Fig. 2f, the sphere has a rough surface with mesoporous structure, which confirms that the spheres are formed through the agglomeration of a large number of small titania crystallites during the solvothermal process.

From Fig. 2a–e, it can be found that the sphere size varies slightly with the thiourea amount. The particles in the sample NST-050 are the most uniform and smallest. The crystal growth can be explained as an oriented attachment growth mechanism [25–28] under solvothermal conditions. Usually, in aqueous system, the hydrolysis rate of Ti-containing precursors (TBOT) is too fast to form titania with regular shape such as sphere [29–31]. In present research, the precursor solution was a quasi non-aqueous system. The formation rate of titania crystallites through the alcoholysis of TBOT was much slower than that through the hydrolysis process. This slow alcoholysis process of TBOT led to the formation of nano-sized TiO_2 crystallites. Then these nano-sized crystallites aggregated isotropically to form the micrometer-sized spheres due to a well-known aggregation mechanism [32,33]. The mesoporous structure was then formed because of the intercrystallite voids originated from the loose aggregation of the nanoparticles. However, besides the spheres, there are still existing nano-sized particles as shown in Fig. 2. It may be due to the reason that the alcoholysis rate is still faster than the aggregation process of the crystallites to form spheres.

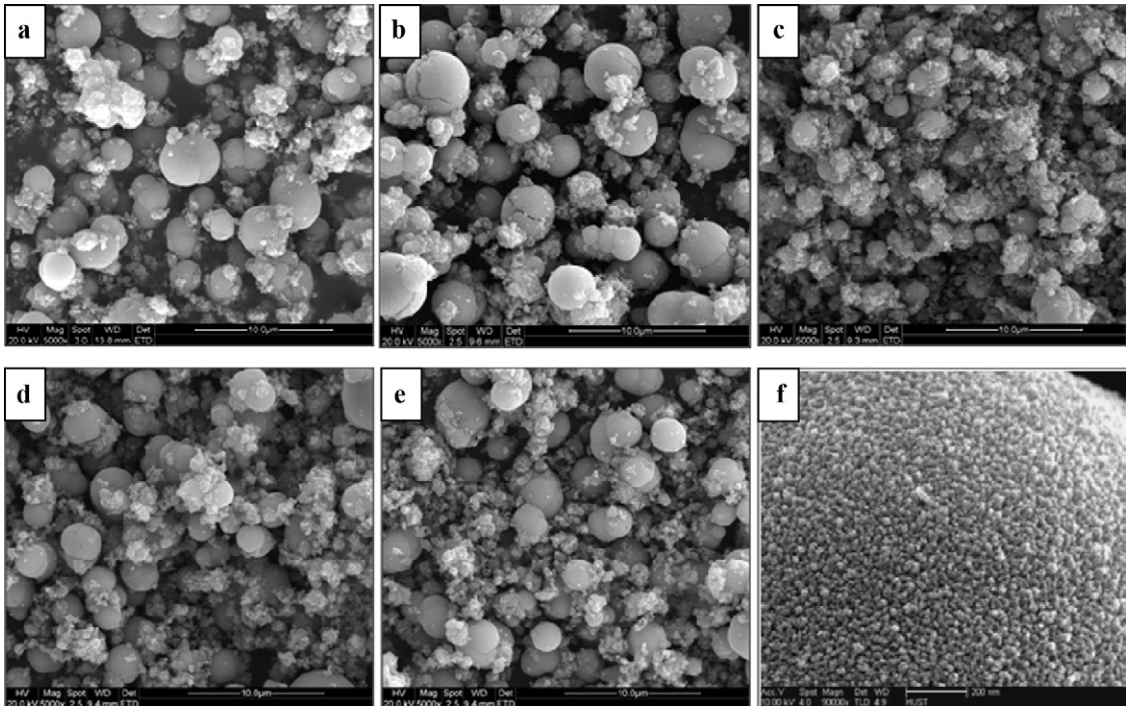

Fig. 2. SEM images of N, S-TiO_2 structure: (a) NST-00, (b) NST-025, (c) NST-050, (d) NST-100, (e) NST-150, and (f) detailed surface of the spheres.

Fig. 3 shows the typical pore size distribution curve from the nitrogen isotherm result by the BJH method of the as-prepared NST-050, which is a type IV isotherm curve with H_2 hysteresis loop, the characteristic of mesoporous materials [34,35]. The formed nanopores have the pore size of about 20 nm. The nitrogen adsorption–desorption isotherms results for all the products are listed in Table 1. It can be found from Table 1 that the doped products have larger surface area than the as-prepared pure TiO_2. This is due to the decomposition of the thiourea during solvothermal treatment, which resulted in the change of pH value of the mixture solution and the formation rate of the crystallites. Also, the partial mesoporous structure of the spheres results in the increase of the surface area, which is helpful for the improvement of the photocatalytic activities. Furthermore, the high surface area is related with the size of the crystallites. With the decrease of the crystallites size calculated from the XRD patterns using Scherrer equation, the surface area of the product increases.

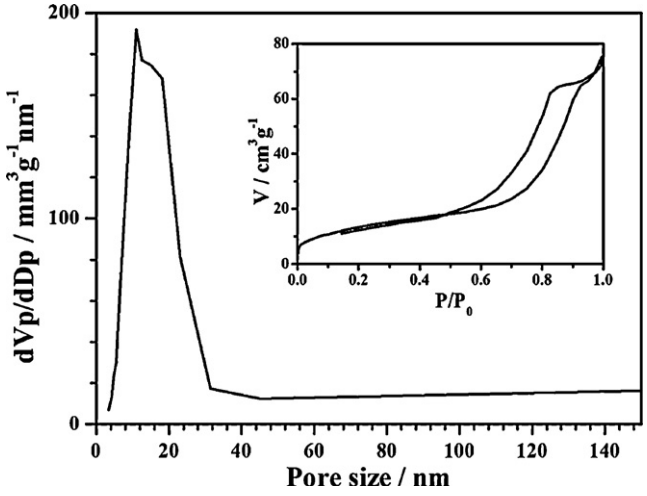

Fig. 3. BJH pore size distribution of the product NST-050 and the corresponding isotherms condition.

The diffuse reflectance spectra of the prepared samples are shown in Fig. 4. The absorption edges of all the doping samples shift to the visible-light region, compared to the pure anatase TiO_2. Among them, the sample NST-025 obviously has the strongest absorption to the visible-light. These results can be attributed to the N and S doping, which can narrow the band gap of the TiO_2 and produce more charge carriers. Thus the enhancement of absorption for the visible-light would be beneficial for the improvement of the photocatalytic ability.

The typical XPS analysis result of the doped TiO_2 NST-050 is shown in Fig. 5. The S 2p data include two peaks in the spectrum around binding energy (BE) of 168.6 eV and 169.7 eV. Researches have indicated that S 2p peaks are found for high oxidation states at BE > 168 eV. Thus these two BE peaks can be attributed to S^{6+} in the lattice replace for Ti^{4+}, meaning the S cationic doping in the lattice [36,37]. No obvious

Table 1
BET surface area and crystallite size of as-prepared products.

Samples	Molar ratio of thiourea/TiO_2	Crystallite size (nm)	S_{BET} (m^2/g)
NST-000	0	46.24/28.83(*r*)	29.11
NST-025	0.25/1	42.05/26.30(*r*)	36.25
NST-050	0.50/1	20.36	65.32
NST-100	1.00/1	33.52	38.04
NST-150	1.50/1	26.07	49.90

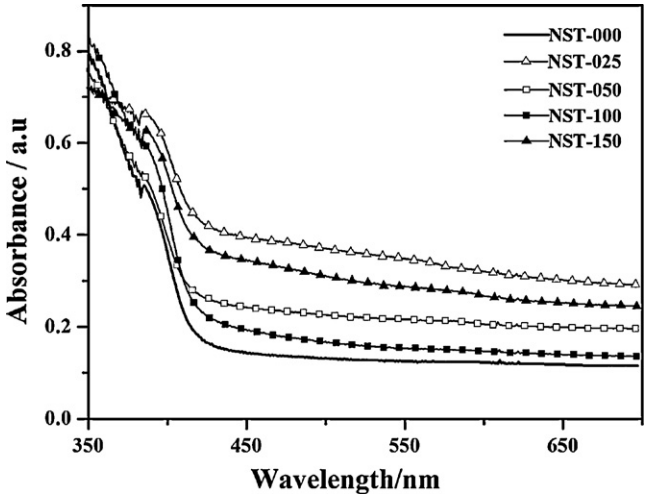

Fig. 4. UV–vis diffuse reflectance spectra of the TiO_2 products.

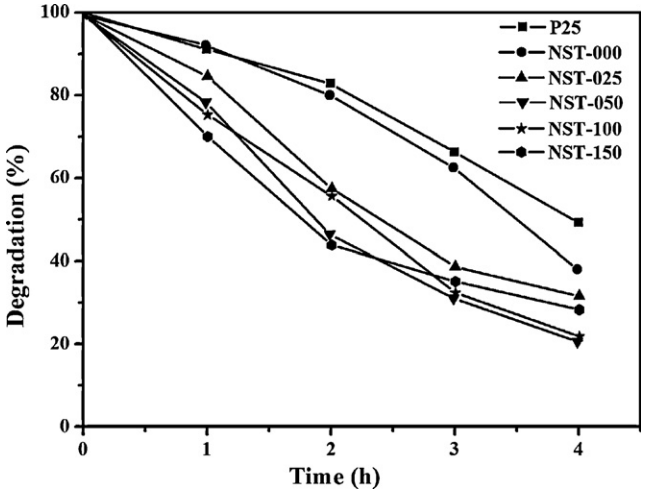

Fig. 6. Photocatalytic activities of TiO_2 products and Degussa P25 under the visible-light irradiation.

S^{2-} ions replacement of O^{2-} ions in the lattice can be observed since there is no peaks locating at around BE 161.8 eV for S^{2-} ions replacing the O^{2-} ions in the lattice of TiO_2, which will cause a lattice distortion for the notable ionic radius difference between S^{2-} (0.184 nm) and O^{2-} (0.140 nm) [38]. The total volume of S doping in NST-050 is about 0.35 at%.

The N1s roughly contains two kinds of peaks at 395.9 eV and 399.7 eV, which is similar with the reported results [39]. The peak detected at 395.9 eV is due to the form of nitrides chemisorbed on the surface of the products, and BE of 399.7 eV is resulted from the formation of O–Ti–N sites in anatase TiO_2 lattice. The total N doping in NST-050 is about 0.62 at%.

The XPS results confirm that N and S elements have successfully incorporated into the lattice of anatase TiO_2. The result is consistent with the theoretical calculation of our previous study result about N and S doped TiO_2 that confirms N replacing O site and S replacing Ti site in anatase lattice [40]. The codoping effect will result in the occurrence of the hybridized states located in the band gap, resulting in the band gap narrowing.

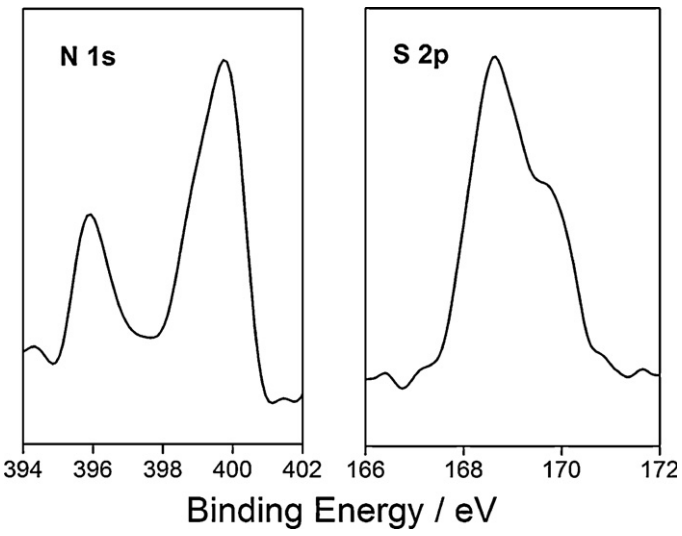

Fig. 5. XPS result of the doped TiO_2 products.

3.2. Photocatalytic activity of (N, S)-codoped TiO_2

In Fig. 6, the photocatalytic activities of the as-prepared TiO_2 products and commercial Degussa P25 TiO_2 nanopowders were evaluated by measuring the degradation efficiency of the MB aqueous solution under visible-light irradiation. The result shows that all the prepared TiO_2 products are superior to Degussa P25 in the visible-light region, regardless of the doping or not. This is because of the codoping effect that would change the gap band of TiO_2. Among them, the NST-050 sample displays the highest photocatalytic activity, which could be ascribed to the synergic effect of its large surface area and (N, S)-doping.

4. Conclusions

Mesoporous structure (N, S)-codoped TiO_2 products have been successfully synthesized through a simple solvothermal method with the thiourea as the resources of N and S. XPS results confirm that N and S have been incorporated into anatase lattice. And the co-doped products exhibits higher photocatalytic activities than the undoped TiO_2 or P25 under the visible-light irradiation, because the codoping can narrow the band-gap of anatase TiO_2.

Acknowledgements

This research was financially supported by National Science Foundation of China under contract No. 50902056, Scientific Research Foundation for the Returned Overseas Chinese Scholars of Ministry of Education, Fundamental Research Funds for the Central Universities (HUST 2010MS087), and the State Key Lab of Material Processing and Die & Mould Technology. The authors would like to thank Materials

Characterization Center of Huazhong University of Science and Technology for XPS and UV–vis assistance.

References

[1] A. Fujishima, K. Honda, Electrochemical photolysis of water at a semiconductor electrode, Nature 238 (1972) 37–38.

[2] A. Mills, S. LeHunte, An overview of semiconductor photocatalysis, J. Photochem. Photobiol. A 108 (1997) 1–35.

[3] N. Wang, C. Zhang, H. He, X. Li, J. Yang, Hydrothermal-assisted liquid phase deposition synthesis and photocatalytic activities of titania nanocrystals, Powder Technol. 205 (2011) 61–64.

[4] N. Wang, L. Han, H. He, N.H. Park, K. Koumoto, A novel high-performance photovoltaic–thermoelectric hybrid device, Energy Environ. Sci. 4 (2011) 3676–3679.

[5] N. Wang, J. Yang, H. He, A novel two-step method to synthesize lotus-leaf-structured TiO_2 nanocrystals with good photocatalytic activity, Powder Technol. 208 (2011) 744–746.

[6] A. Fujishima, T.N. Rao, D.A. Tryk, Photocatalytic degradation of organic compounds over combustion-synthesized nano-TiO_2, J. Photochem. Photobiol. C 1 (2000) 1–21.

[7] B. Chi, T. Jin, Synthesis of titania nanostructure films via $TiCl_4$ evaporation–deposition route, Crystal Growth Des. 7 (2007) 815–819.

[8] M.E. Kurtoglu, T. Longenbach, P. Reddington, Y. Gogotsi, Photoinduced reactivity of titanium dioxide, J. Am. Ceram. Soc. 94 (2011) 1101–1108.

[9] O. Carp, C.L. Huisman, A. Reller, Prog. Solid State Chem. 32 (2004) 33–177.

[10] R. Asahi, T. Morikawa, T. Ohwaki, K. Aoki, Y. Taga, Visible-light photocatalysis in nitrogen-doped titanium oxides, Science 293 (2001) 269–271.

[11] Y.L. Su, Y.T. Xiao, Y. Li, Y.X. Du, Y.L. Zhang, Preparation, photocatalytic performance and electronic structures of visible-light-driven Fe–N-codoped TiO_2 nanoparticles, Mater. Chem. Phys. 126 (2011) 761–768.

[12] D.E. Gu, B.C. Yang, Y.D. Hu, V and N co-doped nanocrystal anatase TiO_2 photocatalysts with enhanced photocatalytic activity under visible light irradiation, Catal. Commun. 9 (2008) 1472–1476.

[13] L.C. Jia, C.C. Wu, S. Han, N. Yao, Y.Y. Li, Z.B. Li, B. Chi, J. Pu, L. Jian, Theoretical study on the electronic and optical properties of (N, Fe)-codoped anatase TiO_2 photocatalyst, J. Alloys Compd. 509 (2011) 6067–6071.

[14] M. Pelaez, A. de la Cruz, E. Stathato, P. Falaras, D. Dionysiou, Visible light-activated N-F-codoped TiO_2 nanoparticles for the photocatalytic degradation of microcystin-LR in water, Catal. Today. 144 (2009) 19–25.

[15] R. Long, N.J. English, Band gap engineering of (N, Ta)-codoped TiO_2: a first-principles calculation, Chem. Phys. Lett. 478 (2009) 175–179.

[16] R. Long, N.J. English, Synergistic effects on band gap-narrowing in titania by codoping from first-principles calculations, Chem. Mater. 22 (2010) 1616–1623.

[17] B. Chi, L. Zhao, J. Li, J. Pu, Y. Chen, C.C. Wu, T. Jin, TiO_2 mesoporous thick films with large-pore structure for dye-sensitized solar cell, J. Nanosci. Nanotechnol. 8 (2008) 3877–3882.

[18] A. Hattori, H. Tada, High photocatalytic activity of F-doped TiO_2 film on glass, J. Sol–Gel Sci. Technol. 22 (2001) 47–52.

[19] R.L. Phen, J.F. Banfield, Morphology development and crystal growth in nanocrystalline aggregates under hydrothermal conditions: insights from titania, Geochim. Cosmochim. Acta 63 (1999) 1549–1557.

[20] D.G. Shchukin, R.A. Caruso, Template synthesis and photocatalytic properties of porous metal oxide spheres formed by nanoparticle infiltration, Chem. Mater. 16 (2004) 2287–2292.

[21] P.D. Yang, D.Y. Zhao, D.I. Margolese, B.F. Chmelka, G.D. Stucky, Generalized syntheses of large-pore mesoporous metal oxides with semicrystalline frameworks, Nature 396 (1998) 152–155.

[22] M. Niederberger, M.H. Bartl, G.D. Stucky, Benzyl alcohol and titanium tetrachloride-A versatile reaction system for the nonaqueous and low-temperature preparation of crystalline and luminescent titania nanoparticles, Chem. Mater. 14 (2002) 4364–4370.

[23] H. Shibata, T. Ogura, T. Mukai, T. Ohkubo, H. Sakai, M. Abe, Direct synthesis of mesoporous titania particles having a crystalline wall, J. Am. Chem. Soc. 127 (2005) 16396–16397.

[24] H.M. Luo, T. Takata, Y.G. Lee, J.F. Zhao, K. Domen, Y.S. Yan, Photocatalytic activity enhancing for titanium dioxide by co-doping with bromine and chlorine, Chem. Mater. 16 (2004) 846–849.

[25] E. Martínez-Ferrero, Y. Sakatani, C. Boissière, D. Grosso, A. Fuertes, J. Fraxedasa, C. Sanchez, Nanostructured titanium oxynitride porous thin films as efficient visible-active photocatalysts, Adv. Funct. Mater. 17 (2007) 3348–3354.

[26] B. Chi, L. Zhao, T. Jin, One-step template-free route for synthesis of mesoporous N-doped titania spheres, J. Phys. Chem. C 111 (2007) 6189–6193.

[27] A. Folli, I. Pochard, A. Nonat, U.H. Jakobsen, A.M. Shepherd, D.E. Macphee, Engineering photocatalytic cements: understanding TiO_2 surface chemistry to control and modulate photocatalytic performances, J. Am. Ceram. Soc. 93 (2010) 3360–3369.

[28] I.N. Seekkuarachchi, H. Kumazawa, Aggregation and disruption mechanisms of nanoparticulate aggregates. 1. Kinetics of simultaneous aggregation and disruption, Ind. Eng. Chem. Res. 47 (2008) 2391–2400.

[29] X.C. Jiang, T. Herricks, Y.N. Xia, Monodispersed spherical colloids of titania: synthesis, characterization, and crystallization, Adv. Mater. 15 (2003) 1205–1209.

[30] U. Jeong, Y.L. Wang, M. Ibisate, Y.N. Xia, Some new developments in the synthesis, functionalization, and utilization of monodisperse colloidal spheres, Adv. Funct. Mater. 15 (2005) 1907–1921.

[31] Y.W. Wang, H. Xu, X. Zhang, H.M. Jia, L.Z. Zhang, J.R. Qiu, A general approach to porous crystalline TiO_2, $SrTiO_3$, and $BaTiO_3$ spheres, J. Phys. Chem. B 110 (2006) 13835–13840.

[32] C. Boissiere, A. van der Lee, A.E. Mansouri, A. Larbot, E. Prouzet, A double step synthesis of mesoporous micrometric spherical MSU-X silica particles, Chem. Commun. (1999) 2047–2048.

[33] M. Ocaña, R. Rodriguez-Clemente, C.J. Serna, Uniform colloidal particles in solution: formation mechanisms, Adv. Mater. 7 (1995) 212–216.

[34] M. Kruk, M. Jaroniec, Characterization of modified mesoporous silicas using argon and nitrogen adsorption, Chem. Mater. 44 (2001) 725–732.

[35] K.S.W. Sing, D.H. Everett, R.A.W. Haul, L. Moscou, R.A. Pierotti, J. Rouquerol, T. Siemieniewska, Reporting physisorption data for gas/solid systems with special reference to the determination of surface area, Pure Appl. Chem. 57 (1985) 603–619.

[36] D.E. Gu, B.C. Yang, Y.D. Hu, V and N co-doped nanocrystal anatase TiO_2 photocatalysts with enhanced photocatalytic activity under visible light irradiation, Cataly. Commun. 9 (2008) 1472–1478.

[37] F.G. Wei, L.S. Ni, P. Cu, Preparation and characterization of N-S-codoped TiO_2 photocatalyst and its photocatalytic activity, J. Hazard. Mater. 156 (2008) 135–140.

[38] R.X. Cai, Y. Kubota, A. Fujishima, Effect of copper ions on the formation of hydrogen peroxide from photocatalytic titanium dioxide particles, J. Catal. 219 (2003) 214–218.

[39] R.L. Phen, J.F. Banfield, A model for exploring particle size and temperature dependence of excess heat capacities of nanocrystalline substances, Nanostruct. Mater. 10 (1998) 185–194.

[40] L.C. Jia, C.C. Wu, Y.Y. Li, S. Han, Z.B. Li, B. Chi, J. Pu, L. Jian, Enhanced visible-light photocatalytic activity of anatase TiO_2 through N and S codoping, Appl. Phys. Lett. 98 (2011) 211903.